A study of microstructure and property of Fe-B-C alloy modified by Ti-Ce-Mg

LI XUEYI*, FU HANGUANG[a], KUANG JIACAI[b], WANG JINTAO[c]
College of Mechanical and Electrical Engineering, Shandong University of Science and Technology, Qingdao 266510, Shandong Province, P. R. China
[a]*School of Materials Science and Engineering, Beijing University of Technology, Beijing 100124, P. R. China*
[b]*Institute of Materials Science and Engineering, Changsha University of Science and Technology, Changsha 410076, Hunan Province, P. R. China*
[c]*National Institute of Metrology, Beijing 100013, Beijing, P. R. China*

Effect of Ti-Ce-Mg compound modification on microstructures, mechanical property and wear resistance of cast Fe-B-C alloy containing 0.25%C, 1.80%B, 0.40%Si, 0.60%Mn and 0.80%Cr has been investigated by optical microscopy (OM), scanning electron microscopy (SEM), and X-ray diffraction (XRD) analysis, hardness test, impact test and wear test. The results indicate that the solidification microstructures of Fe-B-C alloy consist of $Fe_2(B,C)$, $Fe_3(C, B)$, pearlite, and ferrite. $Fe_2(B, C)$ type borocarbide is continuously distributed over the grain boundary. After modification by Ti-Ce-Mg, solidification microstructures of Fe-B-C alloy are obviously refined and there are many obvious necking and broken net in borocarbides. The hardness of modified Fe-B-C alloy has no obvious change comparing with that of unmodified Fe-B-C alloy. Ti-Ce-Mg compound modification can considerably improve impact toughness and wear resistance of cast Fe-B-C alloy.

(Received February 19, 2013; accepted July 10, 2014)

Keywords: Fe-B-C alloy, Ti-Ce-Mg compound modification, Solidification microstructure, Borocarbide, Mechanical property, Wear resistance

1. Introduction

Traditionally, white cast irons (WCI) have been used in applications where high wear resistance is required [1, 2]. In the modern mining applications, the alloys used in crushing and grinding operations need a combination of toughness and wear resistance [1, 2]. Current WCIs, while exhibiting excellent wear properties, have low fracture toughness and are only used in those applications where a limited amount of impact occurs [3, 4]. Over recent years, some researchers have reported that the addition of boron element in the high chromium cast steel can increase the hardness and improve the abrasion resistance of high chromium cast steel. The proper boron concentration in the low alloy cast steel benefits to obtain high hardness boride and improves the wear resistance of Fe-B-C alloy, which also reduces the addition of scarce nickel, molybdenum, chromium and tungsten elements, and therefore decrease the production cost of wear resistant cast steel. Fe-B-C alloy fabricated by adding more than 1.5 % B in the plain carbon steel has high hardness and excellent wear resistance. Its impact toughness is higher than that of WCIs [5-7]. The application of Fe-B-C alloy in high impact work condition results in the decrease of material consumption due to its high abrasion resistance and toughness [8-9].

However, there are many netlike Fe_2B borides in common cast Fe-B-C alloy. Fe_2B boride has high heat stability and is not easy to decompose during the heat treatment. The netlike boride in the Fe-B-C alloy is not favourable to the improvement of the strength and toughness of cast Fe-B-C alloy. Previous many researches discovered that the microstructure and properties of modified cast alloy could increase considerably [10-12]. The purpose of current investigation is to change the netlike borides in Fe-B-C alloy into broken network by adding titanium, rare earth (Ce) and magnesium compound modification, which can increase mechanical property and wear resistance of cast Fe-B-C alloy.

2. Experimental

2.1 The preparation of sample

Fe-B-C alloys were smelted in a coreless laboratory medium frequency induction furnace of 50 kg capability using carburant, low carbon steel, ferroboron, ferrochromium, ferrosilicon and ferromanganese. After being deoxidized with 0.10-0.12%Al from 1600-1620 ^oC, the molten steel was transferred into two pre-heated ladles.

Wherein one of them was modified with Ti-Ce-Mg composite modifier, the other one did not modify. The samples of 22 mm ×22 mm ×110 mm were cast in permanent moulds. Pouring temperatures of molten steel were 1460-1480 ^{o}C,. Final chemical composition of samples was shown in Table 1. The samples were heat-treated at 850^{o}C, 900^{o}C, 950^{o}C, 1000^{o}C, and 1050^{o}C respectively, for 2 h and followed by oil cooling to the room temperature. The temperature of oil was 60-80 ^{o}C. The tempering process of samples was heating at 200°C for 3 h, followed by cooling to the room temperature in still air.

Table 1. Chemical composition of specimens (%, mass fraction).

Serial number	C	B	Cr	Si	Mn	Ti	Ce	Mg	Fe
A_0	0.26	1.80	0.77	0.41	0.62	-	-	-	Bal.
A_1	0.25	1.83	0.79	0.40	0.62	0.52	0.09	0.07	Bal.

2.2 Microstructure examination

The investigation techniques used for cast Fe-B-C alloy microstructure characterization included X-ray diffraction (XRD), optical microscopy (OM), and scanning electron microscopy (SEM). The samples were etched with 5% nital for optical microscopy examination, while a mixture of 5cc HCl, 45cc 4% picral and 50cc 5% nital was used as an etchant for SEM evaluation. XRD was carried on a MXP21VAHF diffractometer with Copper Kα radiation at 40 kV and 200 mA as an X-ray source. The sample was scanned in the 2θ range of 10^{o}-110^{o} in a step-scan mode (0.02^{o} per step). The measurement of volume fraction of borocarbides used a Leica digital images analyzer on the deep etched specimens.

2.3 Mechanical performance tests

Impact toughness tests were performed on a Charpy impact testing device. The specimen was of 20 mm × 20 mm × 110 mm without notch. The macrohardness testing was done using an MW32-HR-150 type hardness tester. The microhardness was measured by using a Vickers microhardness tester and a load of 0.5 N. At least seven indentations were made on each sample under each experimental condition to check reproducibility of the hardness data.

2.4 Sliding wear tests

Wear tests were conducted in a ML-10 type pin abrasion testing machine shown in Fig. 1 [13, 14]. Two different normal loads (4.9 N, and 9.8 N respectively) were applied, the maximum sliding distance was 10.409 m and the sliding speed was 0.1 m.s^{-1} for all the tests. The disk dimension was 30 mm in diameter and 5 mm in thickness. The samples were abraded on a 150 mesh (105μm) quartz cloth disc, and the hardness of quartz was 1180-1210 Hv. The size of the specimens was ∅6 mm × 25 mm. The mass losses were measured by using a scale with 0.1 mg resolution. The wear rates were calculated from the slopes of mass loss versus sliding distance according to references [15, 16].

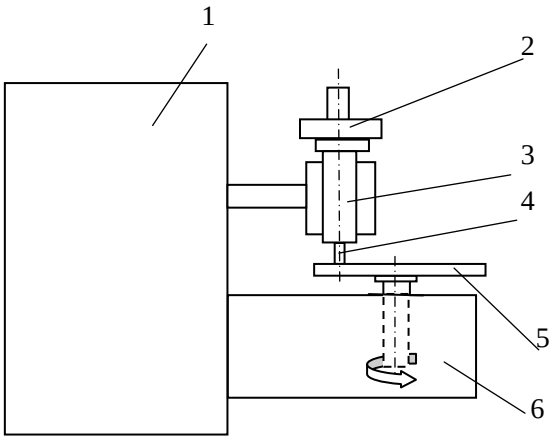

Fig. 1. Schematic drawing of the abrasive wear tester used in this study: 1-controller; 2-load; 3-holder; 4-specimen; 5-disk; 6-revolver.

3. Results and discussion

3.1. As-cast microstructure of Fe-B-C alloy

The solidification microstructures of unmodified Fe-B-C alloy are shown in Fig. 2. Under the common solidification condition, as-cast matrix of unmodified Fe-B-C alloy consists of pearlite and ferrite, and the amount of ferrite is more than that of pearlite. There are many eutectic borocarbides in as-cast structures. The volume fraction of borocarbides is about 12-15 vol.%. The XRD spectrum of Fig. 3 shows that borocarbide in as-cast Fe-B-C sample is Fe_2(B,C) and Fe_3(C, B) type and the amount of Fe_3(C, B) type borocarbide is a few. The micro-harness of Fe_2(B, C) type borocarbides is 1440-1485 Hv, and the micro-harness of Fe_3(C, B) type borocarbides is 930-1015 Hv. The macrohardness of unmodified Fe-B-C sample is 36-39 HRC. Moreover, Fe_2(B, C) type borocarbide is continuously distributed over the grain boundary.

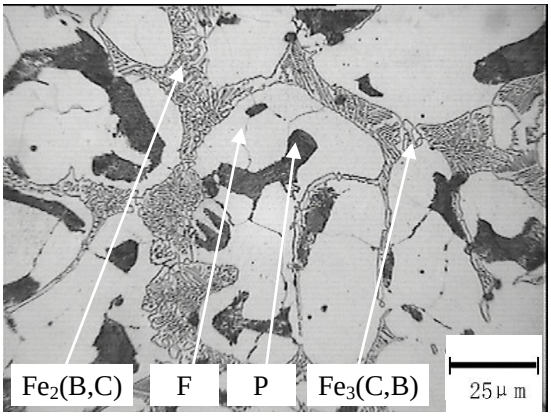

Fig. 2. As-cast microstructure of unmodified Fe-B-C alloy: F-Ferrite, P-Pearlite.

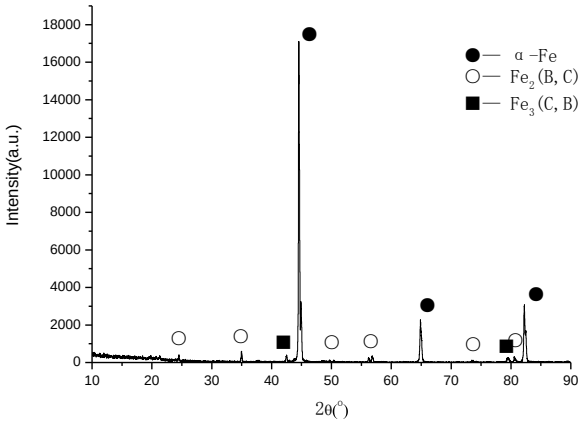

Fig. 3. XRD spectrum of unmodified Fe-B-C alloy.

After modification by Ti-Ce-Mg, the solidification microstructure of Fe-B-C alloy has considerable change. Effects of Ti-Ce-Mg modification on the solidification microstructure of Fe-B-C alloy are shown in Fig. 4. Fig. 5 is its corresponding XRD spectrum. By comparing Fig. 2 and Fig. 4, it can be seen that the solidification microstructures of modified Fe-B-C alloy are obviously refined and there are many obvious necking and broken net in borocarbides. The occurrence of many necking and broken net will promote the improvement of borocarbide morphology in later heat treatment. XRD spectrum of Fig. 5 shows that modified Fe-B-C alloy has $Fe_2(B,C)$ and $Fe_3(C, B)$ type borocarbides and TiB_2 phase. Moreover, as-cast matrix of modified Fe-B-C consists of pearlite, ferrite and martensite. The macrohardness of modified Fe-B-C alloy is 42-45 HRC, and is higher than that of unmodified Fe-B-C alloy.

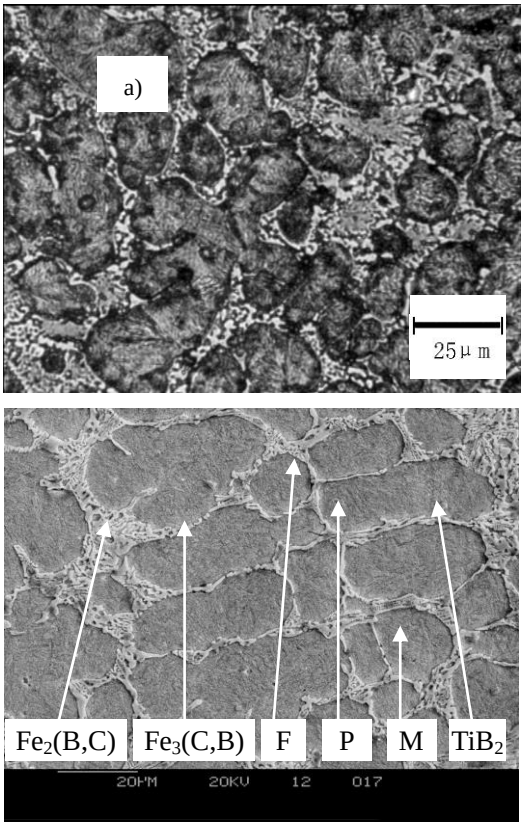

Fig. 4. As-cast OM(a) and SEM(b) of modified Fe-B-C alloy: M-martensite.

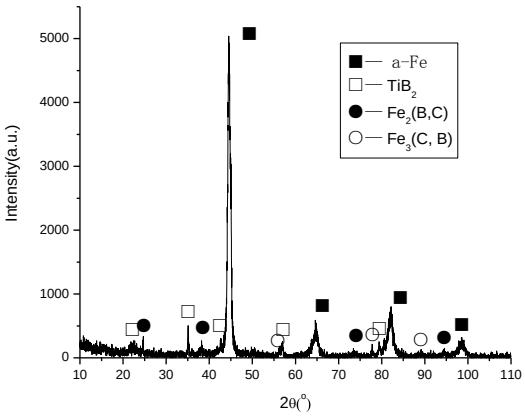

Fig. 5. XRD spectrum of modified Fe-B-C alloy.

When titanium is added into the cast Fe-B-C alloy, the new phase of TiB_2 is formed. However, the TiC and TiB phases do not form, which relates to the thermodynamics and dynamics of the reactions. According to the thermodynamics of the reactions, the reaction equations forming TiC, TiB and TiB_2 are as following [17]:

$$\text{Ti+B=TiB} \quad \Delta G^o = -163200 + 5.9T \ \text{(J/mol)} \quad (1)$$

$$\text{Ti+2B=TiB}_2 \quad \Delta G^o = -284500 + 20.5T \ \text{(J/mol)} \quad (2)$$

$$Ti+C=TiC \quad \Delta G^o = -184800 + 12.55T \ \text{(J/mol)} \qquad (3)$$

From formula (1) to formula (3), it can be seen that the absolute value of reaction free energy forming TiB_2 is the largest, TiB_2 is the most stable in the thermodynamics, so TiB_2 is the easiest to form. According to the dynamics of the reactions, the boron content in the metal melt is much higher than the carbon content, it is easier to form TiB_2 than TiC in the melt. As a result, there is only TiB_2 in the solidification microstructure of modified Fe-B-C alloy and there are no TiC and TiB.

The main reasons that Ti-Ce-Mg improves the solidification microstructure of Fe-B-C alloy are as followings. Rare earth element Ce has low melting point and large atom radius, thereinto, r_{Ce}=0.182nm. Ce and Mg are a strong ingredient undercooling element in the solidification of Fe-B-C alloy. Since the equilibrium constants K_0 are far smaller than 1 [18], the serious segregation occurs during the solidification. A number of elements concentrate in front of the primary austenite through redistribution. This results in high ingredient supercooling, benefits the multiple branching of austenite crystal, reduces the arm space of dendrites and refines the primary austenite [18, 19]. Thus, the dendrite structures and the eutectic borocarbide formed in the residual melts at the end of solidification are all refined. In addition, Ce and Mg can also deoxidize and desulfurize in molten steel, decreasing the contents of sulfur and oxygen by combining them to form Ce_2O_3, Ce_2S_2O, MgS, MgO, and which increases supercooling degree of eutectic solidification and promotes the refinement of eutectic structure [20, 21].

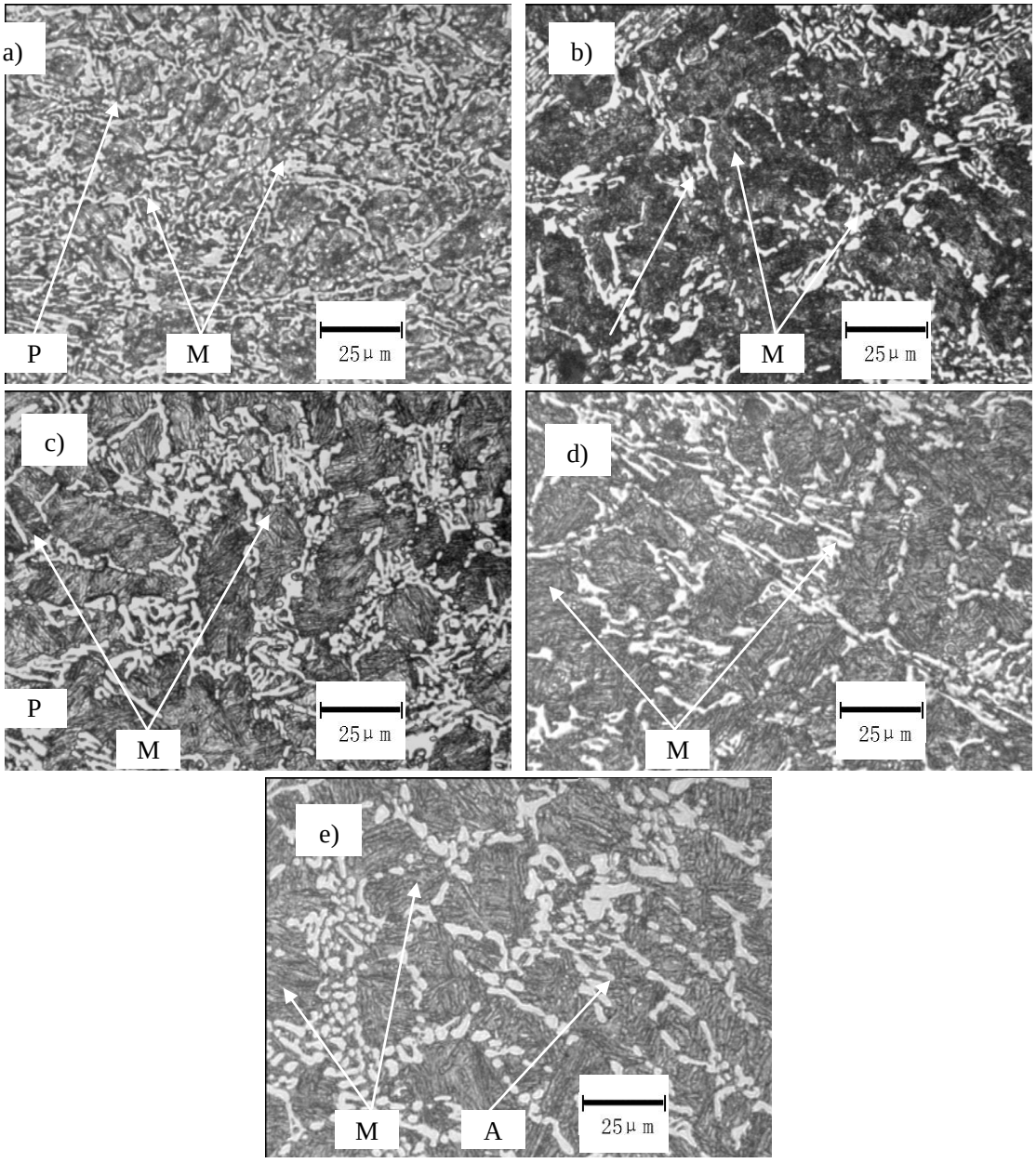

Fig. 6. Quenching microstructure of modified Fe-B-C alloy at different quenching temperature: a) 850 °C; b) 900 °C; c) 950 °C; d) 1000 °C; e) 1050 °C: P-Pearlite, M-Martensite, A-Austenite.

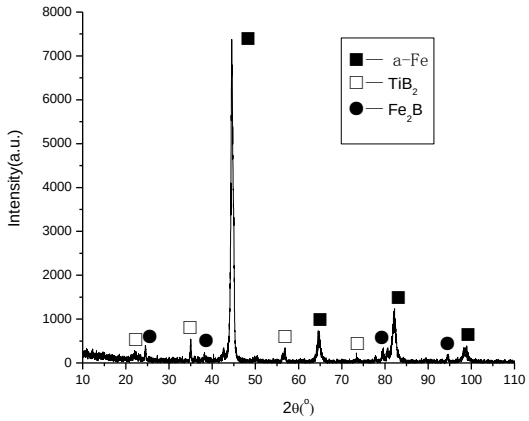

Fig. 7. XRD spectrum of modified Fe-B-C alloy after quenching at 1000 °C.

3.2 Effect of heat treatment on microstructure of Fe-B-C alloy

The effects of quenching temperature on the microstructure of Fe-B-C alloy are shown in Fig. 6. The matrix of Fe-B-C alloy begins to transform the martensite after quenching treatment. The matrix of Fe-B-C alloy all transforms into the martensite when quenching temperature reaches 950 °C, as shown in Figure 6c. Because the carbon concentration in Fe-B-C alloy is lower, the quenching matrix structure of Fe-B-C alloy is all the lath martensite. Moreover, when the quenching temperature reaches 1050 °C, the solution amounts of boron, carbon, chromium, manganese etc. elements increase in the high-temperature austenite and the stability of austenite increases, and there is a few retained austenite in the quenching structures, as shown in Fig. 6e. After quenching treatment, all $Fe_3(C, B)$ borocarbide dissolves into the matrix. However, $Fe_2(B, C)$ borocarbide has excellent thermal stability and does not decompose heating at 850-1050 °C. The XRD spectrum of Fig. 7 shows that borocarbide after quenching is still $Fe_2(B, C)$ type. Part of $Fe_2(B, C)$ borocarbide dissolves into matrix at the weak linking location of borocarbide network, and the local broken borocarbide network appears, when modified Fe-B-C alloy heats at higher temperature, as shown in Fig. 6d-6e.

3.3 Effect of heat treatment on mechanical property and wear resistance of alloy

The effects of heat treatment on hardness and impact toughness of Fe-B-C alloy are shown in Fig. 8 and Fig. 9. When quenching temperature is 850-950 °C, the hardness of Fe-B-C alloy has a considerable increase with the increase of temperature, then the hardness has only a slight increase while exceeding 950 °C, and the hardness has no obvious change when quenching temperature exceeds 1000 °C. When quenching temperature is lower, there is some low hardness pearlite in matrix, so the hardness of Fe-B-C alloy is lower. When quenching temperature reaches 950 °C, matrix all transforms into martensite, which leads to the increase of hardness of Fe-B-C alloy considerably. Moreover, the hardness of cast alloy depends on the hardness of martix and borocarbide volume fraction, modification has no obvious effect on martix and borocarbide volume fraction, so the hardness of modified Fe-B-C alloy has obvious change comparing with that of unmodified Fe-B-C alloy. However, modification has a considerable effect on impact toughness of Fe-B-C alloy as shown in Fig. 9.

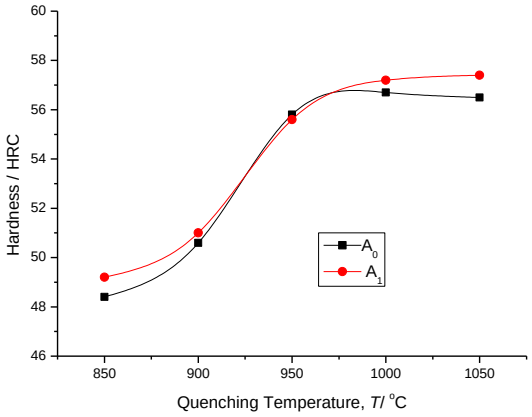

Fig. 8. Effect of quenching temperature on hardness of Fe-B-C alloy: A_0-Unmodified alloy, A_1-Modified alloy.

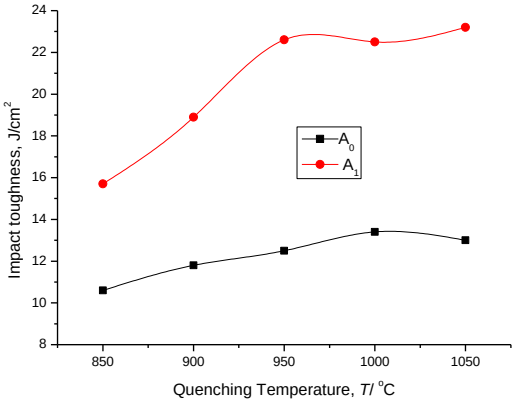

Fig. 9. Effect of quenching temperature on impact toughness of Fe-B-C alloy (Tempering at 200 °C for three hours).

The main reason that Ti-Ce-Mg compound modification improves impact toughness of Fe-B-C alloy is that solidification microstructures of Fe-B-C alloy become obliviously fine after being modified, more borocarbides appear in discontinuous morphology, which is in favour of isolating and spheroidizing of eutectic borocarbides during later heat treatment. Most of the borocarbide network in the modified Fe-B-C alloy is broken and large quantity of granular borocarbides appear after heated to 1000°C; Most of the borocarbides become

granules or spheroidized, and network disappear completely after heated to 1050°C, shown in Fig. 6e. Borocarbide of unmodified Fe-B-C alloy has no obvious change and is continuously distributed over the grain boundary after quenching treatment, as shown in Fig. 10. Fig. 11 shows the fractograph of modified and unmodified cast Fe-B-C alloy. From the observations of ruptured surfaces, it can be seen that there exist secondary cracks at borocarbides as well as interface between eutectic borocarbide and matrix. The ruptured surface of specimen without any Ti-Ce-Mg modification shows mainly inter granular fractured feature, while the ruptured surface of specimen with Ti-Ce-Mg modification is characteristic of both cleavage and inter granular fracture. The reason for the phenomenon above is the difference in the morphology and distribution of borocarbide, this indicates that specimen with Ti-Ce-Mg modification has better toughness than specimen without Ti-Ce-Mg modification.

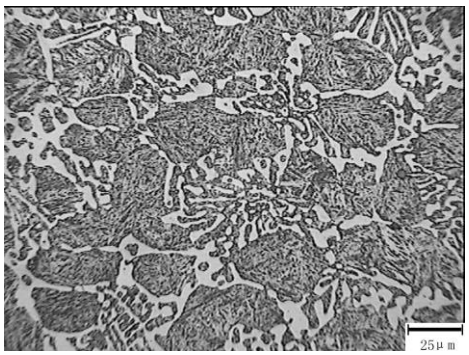

Fig. 10. Microstructure of unmodified Fe-B-C alloy after quenching at 1050 °C.

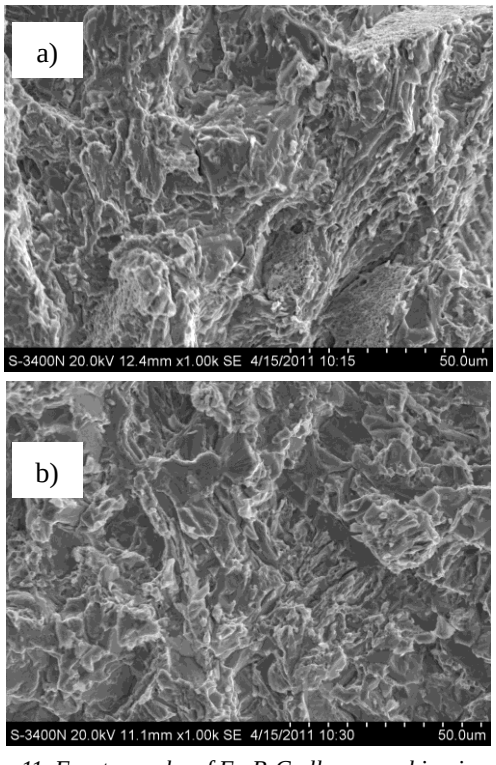

Fig. 11. Fractography of Fe-B-C alloy quenching impact sample at 1050°C and tempering at 200°C before(a) and after(b) modification.

Fig. 12 shows the effect of quenching temperature on the wear resistance of Fe-B-C alloy. The wear resistance of modified Fe-B-C alloy is more excellent than that of unmodified. The wear resistance of alloy at low load (4.9N) is higher than that at high load (9.8N). Moreover, quenching temperature has obvious effect on the wear resistance of Fe-B-C alloy. When quenching temperature is lower, Fe-B-C alloy has lower wear resistance. When quenching temperature reaches 1000 °C, the wear resistance of Fe-B-C alloy is the best, and wear resistance of Fe-B-C alloy has no obvious change while increasing quenching temperature farther. In the wear of materials, the formula for computing the wear rate is given by [22, 23]:

$$W_t = W_c + W_f \tag{4}$$

$$W_c = K_1 \frac{P}{H} \tag{5}$$

$$W_f = K_2 \frac{P}{(\varepsilon_f H)^2} \tag{6}$$

Where W_t is the wear rate of materlals, W_c is the wear rate caused by cutting, W_f is the wear rate caused by fatigue, P is pressure, H is hardness, and ε_f is fracture strain at single axis tensile, which reflects the toughness.

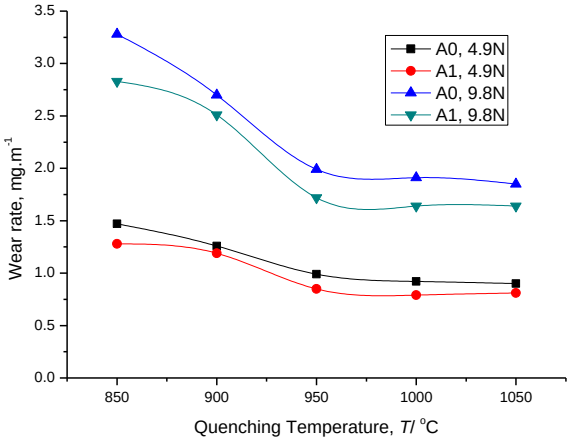

Fig. 12. Effect of quenching temperature on wear resistance of Fe-B-C alloy (tempering at 200°C).

From the above equations, it can be noted that the wear of materials consists of cutting wear and fatigue wear for high-stress abrasion. The former depends on the hardness of materials and the latter is related to the hardness and toughness of materials. As studied earlier, the hardness and toughness are low when quenched at low temperature. The wear resistance of Fe-B-C alloy is therefore low. When quenching temperature increases, the hardness and toughness of Fe-B-C alloy increases also,

which lead to the increase of wear resistance. Moreover, impact toughness of unmodified Fe-B-C alloy is apparently lower, this causes the wear resistance, especially fatigue wear resistance drop to lower level. So the wear resistance of unmodified Fe-B-C alloy is lower than that of modified.

4. Conclusions

1. Solidification microstructure of Fe-B-C alloy containing 0.25%C, 1.80%B, 0.40%Si, 0.60%Mn and 0.80%Cr consists of $Fe_2(B,C)$ and $Fe_3(C, B)$ type borocarbides, pearlite, and ferrite, and the amount of ferrite is more than that of pearlite.

2. After modification by Ti-Ce-Mg, solidification microstructures of Fe-B-C alloy are obviously refined and there are many obvious necking and broken net in borocarbides.

3. The matrix of Fe-B-C alloy all transforms into the martensite when quenching temperature reaches 950 ^{o}C. When quenching temperature is 850-950 ^{o}C, the hardness of Fe-B-C alloy has a considerable increase with the increase of temperature, and the hardness has no obvious change while excelling 1000 ^{o}C.

4. Ti-Ce-Mg compound modification can considerably improve impact toughness and wear resistance of cast Fe-B-C alloy.

Acknowledgement

The authors would like to thank the financial support for this work from the State Key Laboratory for Mechanical Behavior of Materials (Grant No. 20131302), National commonweal research of the Ministry of land and Resources (201411107-8), Beijing Natural Science Foundation (2142009), Scientific Plan Item of Beijing Education Committee under grant (KM201310005003), and the Special funds for cultivation of Taishan Scholars.

References

[1] C. Scandian, C. Boher, J. D. B. de Mello, F. Rézaï-Aria. Wear., **267**, 401 (2009).
[2] J. A. Pero-Sanz, D. Plaza, J. I. Verdeja, J. Asensio. Materials Characterization., **43**, 33 (1999).
[3] C. K. Kim, S. Lee, J. Y. Jung. Metallurgical and Materials Transactions A., **37A**, 633 (2006).
[4] A. Bedolla-Jacuinde, R. Correa, I. Mejía, J. G. Quezada, W. M. Rainforth. Wear, **263**, 808 (2007).
[5] H. G. Fu, Z. W. Wu, J. D. Xing. Materials Science and Technology., **23**, 460 (2007).
[6] J. Hou, H. Fu, Y. Lei, D. Yi, J. Xing. Materialwissenschaft und Werkstofftechnik., **41**, 166 (2010).
[7] J. W. Li, G. S. Zhang, S. Z. Wei, Q. Zhao. Applied Mechanics and Materials., **52-54**, 1718 (2011).
[8] H. G. Fu, D. M. Fu, J. D. Xing. Materials and Manufacturing Processes., **23**, 123 (2008).
[9] X. D. Song, Z. Q. Jiang, H. G. Fu. Foundry Technology., **27**, 805 (2006).
[10] J. Asensio-Lozano, B. Suarez-Pena. Scripta Materialia., **54**, 1543 (2006).
[11] X. H. Zhi, J. D. Xing, H. G. Fu, Y. M. Gao. Materials Science and Technology., **25**, 56 (2009).
[12] A. Bedolla-Jacuinde, S. L. Aguilar, C. Maldonado. Journal of Materials Engineering and Performance., **14**, 301 (2005).
[13] J. D. Bressan, R. A. Schopf. AIP Conference Proceedings., **1353**, 1753 (2011).
[14] J. Rendo´n, M. Olsson. Wear., **267**, 2055 (2009).
[15] J. D. Xing, W. H. Lu, X. T. Wang. In Proceedings of International Conference on Wear of Materials, Reston, Virginia, April 11-14 I983, edited by K. C. Ludema (ASME, New York, 1983) p. 45.
[16] H. M. Wang, Q. Zhang, H. S. Shao. Wear Theory and Anti-Wear Technology. Beijing: Science Press., 162-165 (1993).
[17] E. T. Turkdogan. Physical Chemistry of High Temperature Technology. New York: Academic Press, 1980, 5-26.
[18] G. Y. Liang, J. Y. Su. Cast Metals., **4**, 83 (1991).
[19] H. Li, A. McLean, J. W. Rutter, I. D. Sommerville. Metallurgical Transactions B., **19B**, 383 (1988).
[20] Y. J. Li, Q. C. Jiang, Y. G. Zhao, Z. M. He, X. Y. Zhong. Journal of Rare Earths., **17**, 132 (2000).
[21] A. Bedolla-Jacuinde, S. L. Aguilar, B. Hernandez. Journal of Materials Engineering and Performance., **14**, 149 (2005).
[22] J. M. Li. Abrasion on Metal. Metallurgical Industry Press, Beijing, 1990, 217.
[23] J. M. Tong, Y. Z. Zhou, T. Y. Shen, H. J. Deng. Wear., **135**, 217 (1990).

*Corresponding author: lixueyi07@tsinghua.org.cn